Constraining the intergalactic magnetic field with high-energy *Fermi*-LAT observations of 7 ultra-high-frequency peaked BL Lacertae objects.

NATURAL AND AGRICULTURAL SCIENCES
NATUUR- EN LANDBOUWETENSKAPPE
UFS·UV

B. Bisschoff, B. van Soelen, P.J. Meintjes and K.K Singh

Department of Physics, University of the Free State, Bloemfontein, South Africa
bisschoffb@ufs.ac.za

1. ABSTRACT

Galaxies, galaxy clusters and cosmic voids are separated by large distances of nearly empty space called the intergalactic space. In these large, nearly empty regions a weak magnetic field of strength $B < 10^{-9}$ Gauss of primordial origin is predicted to be present [1-3]. This is called the intergalactic magnetic field (IGMF) and knowledge about its strength, structure, origin and evolution is limited. To fully understand the present, past and to envisage the potential future evolution of the Universe and its processes, it is crucial to understand the strength, size and structure of the IGMF. One promising method of indirectly probing the IGMF is by gamma-ray observations of very high energy emitting blazars [4,6,7,8]. These gamma rays will undergo gamma-gamma absorption due to the interaction with the extragalactic background light (EBL), producing electron-positron pairs that will then upscatter off the cosmic microwave background (CMB). This cascading process will then produce a secondary cascade component at lower energies ($\approx 0.1 - 10$ GeV). However, the IGMF can scatter the electron/positron pairs away and thus attenuating the emission that will be superimposed on the blazars' intrinsic spectrum. This attenuation is highly dependent on the IGMF strength (B_{IGMF}) and the coherence length (λ_{IGMF}). Seven hard and non-variable ultra-high-frequency peaked BL Lacertae (UHBL) sources were selected to be re-analysed, using the *Fermi* Science Tools package (version 1.0.5 released on 05/21/2019) with the improved Pass 8 analysis pipeline [10, 11]. Using previous IACT observations results, the secondary cascade component was modelled using the Monte Carlo ELMAG program of Kachelrieß et al. [12] and the primary and total spectrum components were compared to the *Fermi*-LAT spectrum, allowing constraints to be placed on the strength of the IGMF.

2. HE & VHE SPECTRUM MODELLING

Fermi-LAT Pass 8 data for (2008/09/01 – 2018/09/01) between 0.1 and 300 GeV have been downloaded for seven hard and non-variable blazar sources [13]. These sources were re-analysed, by producing light curves and SEDs, to test for variability and obtain their spectral model parameters with the new *Fermi* Science Tools package (version 1.0.5 released on 05/21/2019). All sources within a region of interest (ROI) of 10 degrees from the centre, with a maximum zenith angle of 90 degrees, where considered while performing the model fit with GTLIKE. For the background subtraction the galactic diffuse (gll_iem_v06.fits) and extragalactic isotropic (iso_P8R3_SOURCE_V2.txt) emission template files were also included in the source model file.

Since the secondary cascade component should be most prominent in the $\approx 0.1 - 10$ GeV energy range [4-9], a second, independent *Fermi*-LAT analysis was performed to obtain a power-law (PL) model for this energy range. For two sources, RBG J0152+017 and 1ES 0229+200, the *Fermi*-LAT analysis was done in the $\approx 1 - 10$ GeV energy range because of high photon contamination below 1 GeV. Within this energy range, the spectrum is either a superposition of both the primary intrinsic source spectrum and the secondary cascade spectrum or is only due to the total contribution from the primary intrinsic source spectrum when the secondary cascade component contribution is negligible.

Next a third *Fermi*-LAT analysis was undertaken between $\approx 10 - 300$ GeV to obtain the PL model for the primary intrinsic source spectrum, since the primary spectrum should be the most prominent contributor in this energy range [4-9]. This specific energy range was chosen such that the cascade contribution and the EBL absorption is minimal. This energy range was also chosen such that the Likelihood fit found convergences and that the TS value is above 25 ($\approx 5\sigma$). If these conditions could not be met, the primary spectrum was modelled with a PL or broken power law (BPL) model fitted to the HE data points, as was done for the two sources 1ES 1218+304 and RBG J0152+017.

The VHE data for each source were deabsorbed with the EBL absorption code created by M. Meyer [14]. The spectral parameters of the VHE emission was obtained by fitting a PL model to the VHE data.

Table 1: The seven selected hard and non-variable UHBL sources and all their obtained fitted spectral indexes.

Source	Redshift	VHE data	Power Law Index (0.1 - 10 GeV)	Chosen energy range between 10 – 300 GeV	Broken Power Law Indexes		Power Law Index (0.1 – 300 GeV)
					Index 1	Index 2	
1ES 0414+009	0.287	[16]	1.990 ± 0.119	10 – 100	1.729 ± 0.272	1.855 ± 0.306	1.850 ± 0.032
1ES 0347−121	0.188	[17]	1.762 ± 0.204	10 – 100	1.273 ± 0.404	1.867 ± 0.153	1.656 ± 0.037
1ES 1101−232	0.186	[18]	1.831 ± 0.149	10 – 100	1.208 ± 0.314	1.763 ± 0.165	1.682 ± 0.023
1ES 1218+304	0.182	[19]	1.714 ± 0.034	10 – 40	1.638 ± 0.190	2.151 ± 0.111	1.638 ± 0.190
1ES 0229+200	0.140	[20]	1.775 ± 0.239	10 – 40	1.151 ± 0.675	1.654 ± 0.120	1.720 ± 0.034
RGB J0710+591	0.125	[21]	1.680 ± 0.122	10 – 60	1.366 ± 0.320	1.901 ± 0.185	1.727 ± 0.025
RBG J0152+017	0.080	[22]	1.955 ± 0.297	10 – 60	1.720 ± 0.206	2.404 ± 0.103	1.884 ± 0.052

The intrinsic, primary spectrum from the source was modelled by fitting a BPL to the HE and VHE data, where the photon indexes (Γ_1 and Γ_2) were held at the values obtained from the *Fermi*-LAT analysis and the PL fit to the VHE data.

For comparison to the BPL model, a PL model was also fit to the HE and VHE data.

Table 1 summarizes the results for all seven sources.

3. CASCADE SPECTRUM MODELLING

Monte Carlo simulations were performed to produce the secondary cascade component, using the code that was created and published by Kachelrieß et al. [23]. The code takes as input a BPL spectrum with N number of photons and computes the probability for the photons to go through the cascading process. The input spectrum was modelled as a PL:

$$F(E) = \left(\frac{E}{E_b}\right)^{\Gamma-1} \log\left(\frac{E_{max}}{E_{min}}\right) \frac{E(n_{bin}-1)}{\log(E_{max}/E_{thr})} \quad (1)$$

where E is the energy (eV), Γ is the photon index, E_b is the break energy, E_{max} is the maximum energy, $Emin$ is the minimum energy, E_{thr} is the output cascade threshold energy and n_{bin} is the number of energy bins.

The code also takes the IGMF strength and coherence length as input parameters, and contains 6 different input EBL models from which the Kneiske et al. [25] lower limit model was used to model the cascade spectrum [27].

The output spectrum consists of two different components: the HE cascade spectrum and the VHE observed spectrum. The HE cascade spectrum consists of the photons that went through the cascading process and that were scattered into the lower energy bins ($\lesssim 300$ GeV).

The HE and VHE gamma-ray emission is modeled as a point-like emission, since there has been no evidence found for extended gamma-ray emission around blazar sources thus far [24]. Therefore, photons that get scattered outside the *Fermi*-LAT or IACT point spread function will not be included in the output cascade spectrum by the code.

4. RESULTS

Preliminary constraints could be placed on the IGMF strength by considering three different scenarios: primary dominating flux (lower limit); cascade dominating flux (lower limit) and an intermediate (best-fit) scenario.

Intermediate regime: The HE cascade spectrum was added to the primary intrinsic source spectrum in the HE range ($0.1 - 300$ GeV), obtained from the *Fermi*-LAT analysis, to obtain the total spectrum of the source. The total spectrum was then fitted to the *Fermi*-LAT PL model in the $0.1 - 10$ GeV range. The total flux was not allowed to vary more than one standard deviation from the *Fermi*-LAT HE PL spectrum model.
Cascade regime: In this regime only the cascade spectrum was fit and was not allowed to exceed the *Fermi*-LAT data (in the $0.1 - 10$ GeV range) by more than one standard deviation. The minimum IGMF strength value which satisfied this condition was used as the lower limit for the cascade regime.
Primary regime: A PL/BPL was fitted through the HE and VHE data to obtain the full fit primary spectrum. The total spectrum was then not allowed to exceed the upper error of the full fit primary spectrum. The minimum IGMF strength value which satisfied this condition was used as the lower limit for the primary regime.

Each modelled cascade spectrum was produced for a specific IGMF strength for every fit, for a coherence length of 1 Mpc. All the obtained IGMF strength values for all the sources are shown in table 2 for the best fit and the lower limits for the cascade spectrum dominant case and the primary spectrum dominant case. These values were then used to model the IGMF at the present epoch as [1-3],

$$B_{IGMF} = B_0(1+z)^2 \quad (2)$$

where z is the redshift and B_0 is the IGMF strength at $z = 0$.

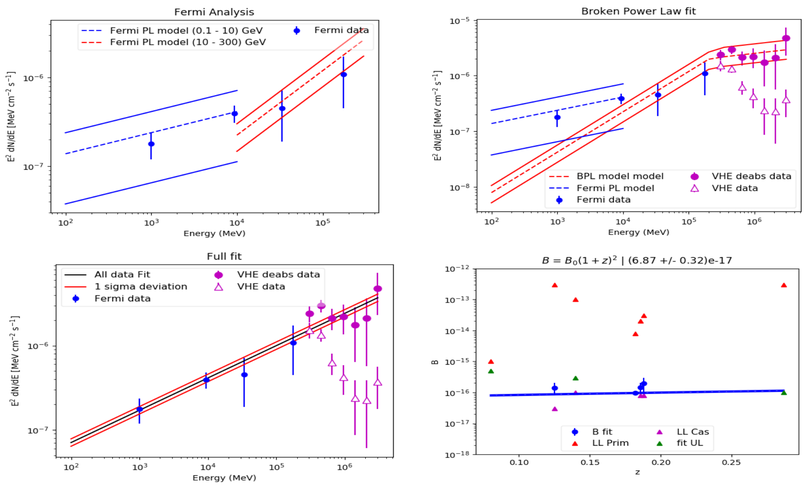

FIGURES on the LEFT hand side:

Top left: *Fermi*-LAT analysis results for a PL fit in the $0.1 - 10$ GeV range (blue line) and in the $10 - 300$ GeV range (red line) through the *Fermi*-LAT data points (blue dots), for the source 1ES 0347-121.
Top right: BPL chi-squared fit for the primary spectrum (red line) through the HE (blue dots) and VHE data (pink dots/triangles) of the source 1ES 0347-121.
Bottom left: PL chi-squared fit for the full primary spectrum (black/red line) through the HE (blue dots) and VHE data (pink dots/triangles) of the source 1ES 0347-121.
Bottom right: IGMF evolution model (equation 2; blue line) with lower limits for both cascade (magenta) and primary (red) dominating spectrum scenarios, for all the sources. The best-fit values are shown as blue data points, while the green triangles indicate the upper error value obtained for the best-fit scenario (see table 2).

FIGURES on the RIGHT hand side:
The input spectrum (cyan) and output cascade spectrum (green) for all sources. The primary spectrum (red) added to the cascade spectrum results in the total spectrum (black) which should be compared to the observed *Fermi*-LAT data (blue points) and PL model (blue line). Note the shaded regions (green and black) represent the 1σ deviation in the VHE primary spectrum (cyan dashed line), which was used as input for the cascade simulations. Only the obtained results from the intermediate regime are shown.

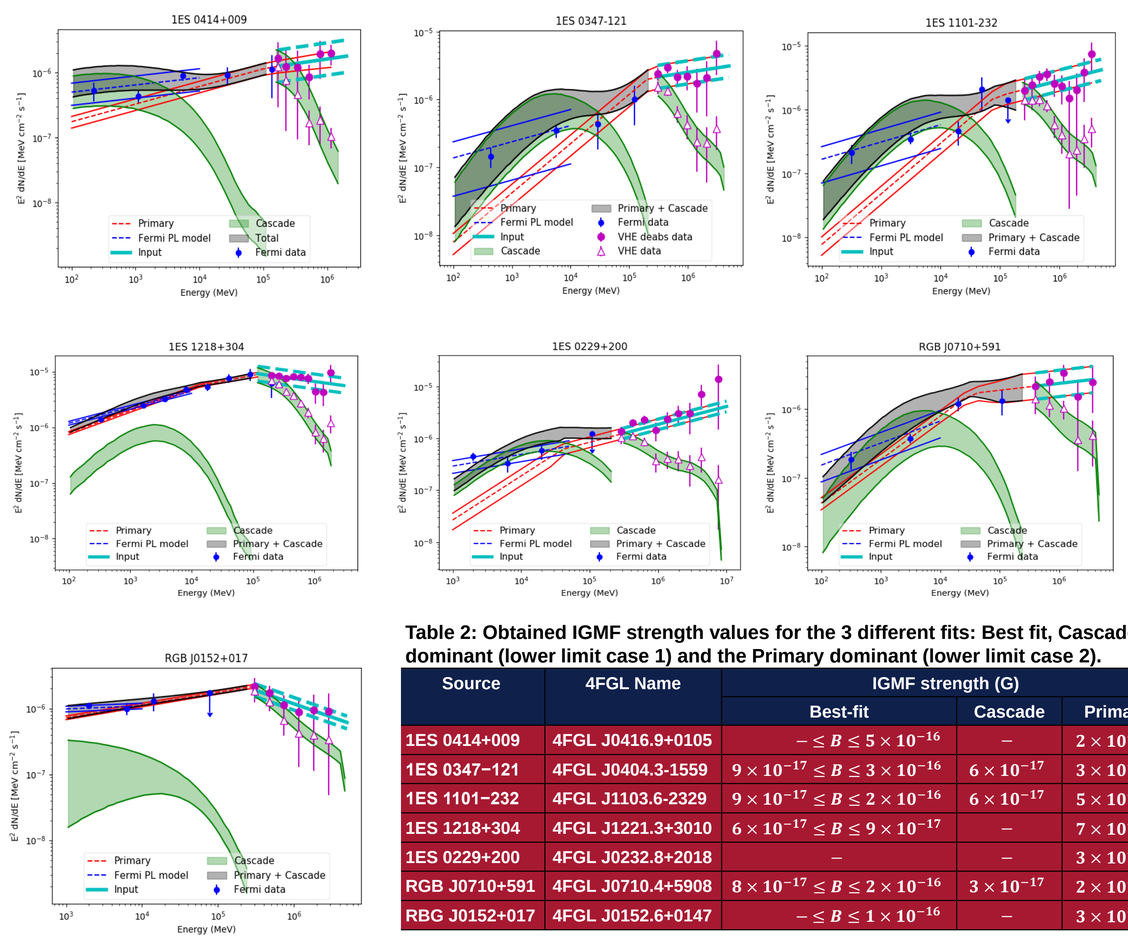

Table 2: Obtained IGMF strength values for the 3 different fits: Best fit, Cascade dominant (lower limit case 1) and the Primary dominant (lower limit case 2).

Source	4FGL Name	IGMF strength (G)		
		Best-fit	Cascade	Primary
1ES 0414+009	4FGL J0416.9+0105	$-\leq B \leq 5\times10^{-16}$	–	2×10^{-15}
1ES 0347−121	4FGL J0404.3-1559	$9\times10^{-17} \leq B \leq 3\times10^{-16}$	6×10^{-17}	3×10^{-14}
1ES 1101−232	4FGL J1103.6-2329	$9\times10^{-17} \leq B \leq 2\times10^{-16}$	6×10^{-17}	5×10^{-15}
1ES 1218+304	4FGL J1221.3+3010	$6\times10^{-17} \leq B \leq 9\times10^{-17}$	–	7×10^{-15}
1ES 0229+200	4FGL J0232.8+2018	–	–	3×10^{-14}
RGB J0710+591	4FGL J0710.4+5908	$8\times10^{-17} \leq B \leq 2\times10^{-16}$	3×10^{-17}	2×10^{-15}
RBG J0152+017	4FGL J0152.6+0147	$-\leq B \leq 1\times10^{-16}$	–	3×10^{-15}

5. CONCLUSION

The HE PL models for the primary spectrum, that were obtained for the *Fermi*-LAT analysis in a specific energy range (between $10 - 300$ GeV) satisfied all the conditions mentioned in section 2. The HE indexes and break energy values obtained for the BPL primary spectrum are in good agreement with Arlen et al. [2]. In the cascade flux dominating regime the minimum lower limit value, of $B_{IGMF} \gtrsim 6\times10^{-17}$ G for redshift $z = 0.188$, gave the most constraining IGMF strength lower limit which, consequently, gives a lower limit for the IGMF strength, at the present epoch, of $B_0 \gtrsim 4\times10^{-17}$ G. This agrees well with the lower limits of $B_{IGMF} \gtrsim 10^{-19}$ G and $B_{IGMF} \gtrsim 3\times10^{-17}$ G , obtained by Finke et al. [4] and Tanaka et al. [5]. In the primary flux dominating regime the most constraining lower limit found was the minimum IGMF strength value, of $B_{IGMF} \gtrsim 2\times10^{-15}$ G for redshift $z = 0.287$, which results in present epoch lower limit of $B_{IGMF} \gtrsim 10^{-15}$ G. This agrees well with the lower limit of $B_{IGMF} \gtrsim 10^{-15}$ G [8,9]. In the intermediate regime, if the HE part of the BPL spectrum (with Index Γ_1), that was obtained from the *Fermi*-LAT analysis in the $10 - 300$ GeV range, does indeed represent the actual primary intrinsic source spectrum then the best-fit value for the present day IGMF strength is $B_0 = (6 \pm 1)\times10^{-17}$ G. Alternative processes that can influence the HE cascade spectrum, such as plasma beam instabilities and anxion-like particle oscillations [30,31], were not considered.

7. ACKNOWLEDGEMENTS

I would like to thank the organizers for the invitation to present my M.Sc. work at this conference. The financial assistance of the National Research Foundation (NRF) towards this research is hereby acknowledged. Opinions expressed and conclusions arrived at, are those of the author and are not necessarily to be attributed to the NRF.

6. REFERENCES

[1] D. Grasso et al., physrep 348 (2001) 3
[2]K. Subramanian, Reports on Progress in Physics 79 (2016) 7
[3] T. Vachaspati, arXiv e-prints (2020), eprint: 2010.10525
[4] Finke J D et al. 2015 Astrophysical Journal Letters 814 1
[5] Y.T. Tanaka et al., ApJ 787 (2014) 2
[6] Vovk I et al. 2012 Astrophysical Journal Letters 747 1
[7] Dermer C D et al. 2011 Astrophysical Journal Letters 733 2
[8] Taylor A M, Vovk I and Neronov A 2011 Astronomy and Astrophysics 529
[9] F. Tavecchio et al., MNRAS 414 (2011) 4
[10] Costamante L et al. 2018 MNRAS 477 3
[11] Kaufmann S G et al. 2019 Multiwavelength view of the TeV Blazar RGB J0152+017.
[12] Kachelrieß M et al. 2012 Computer Physics Communications 183 4
[13] https://fermi.gsfc.nasa.gov/cgi-bin/ssc/LAT/LATDataQuery.cgi
[14] https://github.com/me-manu/eblstud
[15] Urry C et al. 1995 Astronomical Society of the Pacific 107 803
[16] H.E.S.S. Collaboration et al. 2012 Astronomy & Astrophysics 538
[17] Aharonian F et al. 2007 Astronomy and Astrophysics 473 3
[18] Aharonian F et al. 2007 Astronomy and Astrophysics 470 2
[19] Acciari V A et al. 2010 The Astrophysical Journal Letters 709 2
[20] Aharonian F et al. 2007 Astronomy and Astrophysics 475 2
[21] Acciari V A et al. 2010 The Astrophysical Journal Letters 715 1
[22] Aharonian F et al. 2008 Astronomy and 481
[23] http://elmag.sourceforge.net
[24] M. Ackermann et al., ApJS 237 (2018) 2
[25] Kneiske T M and Dole H 2010 Astronomy and Astrophysics 515
[26] Franceschini A, Rodighiero G and Vaccari M 2008 Astronomy and Astrophysics 487 3
[27] Singh K K et al. 2014 New Astronomy 27
[28] Arlen T C et al. 2014 The Astrophysical Journal 796 1
[29] Pshirkov M S et al. 2016 Physical Review Letters 116 19
[30] Ajello M 2016 Physical Review Letters 116 16
[31] Vafin S J et al. 2019 The Astrophysical Journal 873 10
[32] Bray J D et al. 2018 The Astrophysical Journal 861 1
[33] Govoni F et al. 2019 Science 364 6444

bisschoffb@ufs.ac.za | **www.ufs.ac.za**
UFSUV | UFSweb | UFSweb

9th International Fermi Symposium
Virtual Conference
Johannesburg, South Africa, 12th – 17th April, 2021

Fisika - Physics
ASTROPHYSICS UFS
UNIVERSITY OF THE FREE STATE
UNIVERSITEIT VAN DIE VRYSTAAT
YUNIVESITHI YA FREISTATA
UFS·UV
NATURAL AND AGRICULTURAL SCIENCES
NATUUR- EN LANDBOUWETENSKAPPE
Inspiring excellence. Transforming lives.
Inspireer uitnemendheid. Verander lewens.